

A highly miniaturized NDIR methane sensor

N. Pelin Ayerden^a, Ger de Graaf^a, Peter Enoksson^b, and Reinoud F. Wolffenuettel^a

^aFaculty of EEMCS, Delft University of Technology, Mekelweg 4, 2628 CD, Delft, Netherlands

^bMicro and Nanosystems, MC2, Chalmers University of Technology, SE-412 96, Gothenburg, Sweden

ABSTRACT

The increasing demand for handheld systems for absorption spectroscopy has triggered the development of microspectrometers at various wavelength ranges. Several MEMS implementations of the light source, interferometer/optical filter, and detector have already been reported in the literature. However, the size of microspectrometers is still limited by the required absorption path length in the sample gas cell. This paper presents a compact MEMS linear-variable optical filter (LVOF) where the resonator cavity of the filter is also used as a sample gas cell to measure the absorption of methane at 3392 nm wavelength. The physical resonator cavity length is elongated 62.2-fold, using multiple reflections from highly reflective Bragg mirrors to achieve a sufficiently long effective optical absorption path. Although the LVOF would in principle enable operation as a robust portable microspectrometer, here it is used in a miniaturized NDIR methane sensor for wavelength selection and calibration.

Keywords: Optical sensor, spectroscopy, mid-IR, Bragg mirror, Fizeau, methane, gas sensor

1. INTRODUCTION

Optical absorption spectroscopy is a self-referencing and nondestructive material identification method that measures the absorption of light passing through a sample.¹ The composition of the sample is extracted by comparing the measured absorption spectrum to a database. Due to its simple measurement technique and data analysis, optical absorption spectroscopy is highly suitable for portable applications.

The key component in an optical absorption spectrometer is the wavelength-selective element. Wavelength selection can be done either by using a tunable laser as the light source or combining a broadband light source with a wavelength-selective component. Despite their high beam quality and narrow linewidth, tunable lasers in the intended wavelength range, i.e. mid-IR, require the integration of many optical components and the available systems are far from miniaturization at the chip-level.^{2,3} There are several options for wavelength-selective elements to be combined with a broadband light source. Microelectromechanical system (MEMS) implementations of the Michelson^{4,5} and lamellar grating^{6,7} interferometers used in Fourier transform infrared spectrometers have been presented in the literature. However, the operation principle of these devices relies on the optical path difference between a stationary and a movable mirror. Although these devices have high resolution in a wide wavelength range, the vertical arrangement of the mirrors does not allow for bottom-up integration with the rest of the components. Moreover, moving components in a portable instrument reduces the robustness. Dispersion-based miniaturized spectrometers with stationary⁸ and scanning⁹ gratings have been reported in the literature. However, the resolution of grating based microspectrometers is limited by the decreasing dimensions, rendering them unsuitable for demanding portable applications.¹⁰

Miniaturization of spectrometers while maintaining the wideband operating range, high resolution and robustness of their benchtop counterparts is challenging. Interference filter-based microspectrometers offer a significant reduction in size and improvement in robustness at the expense of a limited wavelength range.^{11,12} Interference filters, usually referred to as Fabry-Perot (FP) filters, are composed of two parallel mirrors with a resonator layer in-between. The thickness of the resonator determines the wavelength to be transmitted through the filter. For wideband operation of the FP filter, either one of the mirrors is translated electrostatically,¹³ or an array

Corresponding author: N. Pelin Ayerden. Tel: +31 (0)15-27-87548. E-mail: n.p.ayerden@tudelft.nl.

of filters with different resonator thickness is fabricated.¹⁴ An electrostatically actuated FP filter, i.e. tunable FP filter, is highly sensitive to the flatness of the mirrors and is, therefore, not suitable for portable applications where the device is subject to vibrations. In the case of the static array of filters, mirror flatness ceases to be an issue. Nevertheless, fabrication of a high number of filters to achieve a higher spectral resolving power becomes too complex in this configuration.

An innovative wavelength-selective device, the linear variable optical filter (LVOF), provides wideband operation with high resolving power, while maintaining the robustness without any moving parts. The LVOF is composed of one flat and one tilted mirror, usually at an angle of $\alpha < 50$ millidegrees, with a tapered resonator layer in-between. The thickness of the layer changes linearly along the length of the filter; thereby, creating a continuous array of FP filters. Therefore, when integrated to a detector array, a wideband spectral response can be measured with the LVOF.

According to the Beer-Lambert Law, the absorption of a light beam passing through a sample is a linear function of the optical path length in the sample cell, as well as the absorption coefficient and the concentration of the individual components in a sample.¹⁵ Therefore, the low concentration of a sample can be compensated by a long absorption path for detection. Multipass absorption cells with a combination of spherical mirrors, such as the White cell¹⁶ and the Herriott cell,¹⁷ were the first to elongate the optical absorption path using multiple reflections. Moreover, Thoma *et al.* introduced the circular multipass cell that allows a star-shaped trajectory of the light beam.¹⁸ However, the alignment of the optical mirrors requires stable mechanics, rendering these instruments undesirable, especially for portable applications. Cavity enhanced absorption spectroscopy (CEAS) overcomes this problem by exploiting the multiple reflections in high-finesse optical cavities.¹⁹ The concept of using an absorbing medium in a high-finesse cavity for spectral analysis was first introduced by Jackson²⁰ for spherical FP interferometers and was later discussed by Kastler²¹ for parallel-mirror configurations. Hernandez²² investigated the effect of an absorbing medium in FP interferometers and concluded that extreme high-finesse reflective coatings would be required to achieve a long path cell behavior. Thanks to the advances in microfabrication technology, it is now possible to fabricate highly reflective dielectric mirrors with negligible surface roughness and waviness. Several examples of CEAS devices have been reported with meters of effective optical absorption path at parts-per-billion (ppb) detection levels.^{23,24} However, these instruments require the use of a laser as a light source due to the high power that is necessary to enter a resonator with > 99.99 mirror reflectivity and high optical quality of the beam, such as collimation.

A highly miniaturized spectrometer necessitates the functional integration of the light source, wavelength-selective device, sample cell and the detector. The light source is usually integrated at the component-level to allow for thermal isolation. Monolithic integration of the wavelength-selective device and the detector using MEMS technology has previously been presented for tunable and an array of fixed FP filters.^{25,26} However, in all these implementations, the sample cell remains to be a separate external component. In this paper, we present the functional integration of an LVOF and a gas cell at the chip-level. The resonator cavity of the LVOF is used as a gas cell, exploiting the multiple reflections between highly-reflective mirrors for absorption similar to the CEAS operation principle, while selecting the wavelength. However, in the gas-filled LVOF, more reasonable values for the mirror reflectivity are used, so that a low-cost light source can still be employed, while elongating the μm -level physical cavity length to the mm -level effective optical absorption path. Combining the wavelength selection and optical absorption in one device at a wide wavelength range makes the gas-filled LVOF a significant step in the miniaturization of spectrometers.

2. GAS-FILLED LVOF DESIGN

The gas-filled LVOF is composed of one flat and one tapered Bragg mirror, with a tapered air-gap in-between as shown in Fig. 1. The flat mirror is deposited in a cavity on the bottom wafer, while the tapered mirror is fabricated on the top Si-wafer. These mirrors are subsequently integrated by direct bonding of the top and bottom wafers. Due to the cavity depth on the bottom wafer and the tapered profile of the mirror on the top wafer, a tapered cavity is achieved.

The final device includes two identical gas-filled LVOFs, one sealed and one with openings on both sides of the filter to allow for the gas flow. The sealed LVOF serves as a reference, while the measurement is performed using

the device with the gas inlet and outlet. Therefore, the ambient gas composition is measured without sample preparation or extra equipment to control the sample flow. Moreover, thanks to the self-referencing property, the device does not require periodic calibration.

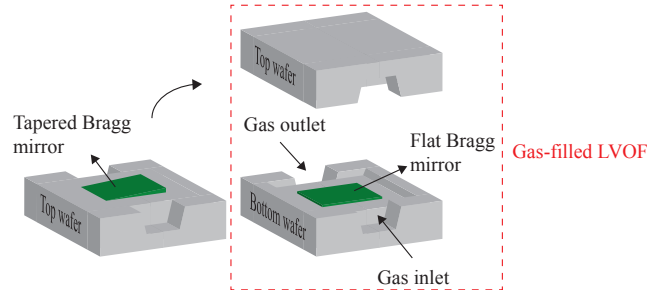


Figure 1. Schematic illustration of the device.

The use of LVOF cavity as a gas cell requires highly reflective mirrors to elongate the optical path through multiple reflections. Quarter-wave Bragg mirrors are well known to provide high reflectivity comparable to metallic coatings. With the right choice of non-absorbing materials they can be used in transmissive optical filters. Bragg mirrors are composed of alternate layers of high and low refractive index materials with quarter wavelength optical thickness. Considering the fabrication tolerance of the film deposition and its effect on the mirror reflectivity, starting with a long physical resonator cavity provides a higher chance of achieving sufficient absorption in the device. However, a long resonator cavity translates into a high order of operation and limits the operating wavelength range, i.e. full spectral range (FSR), of the filter. The device presented here is intended to measure hydrocarbons. These gases have fingerprint regions in $3.1\text{ }\mu\text{m}$ to $3.7\text{ }\mu\text{m}$ wavelength range.

However, selecting such a wide wavelength range limits the operating order to $m = 4$, thereby restricting the cavity length to less than $10\text{ }\mu\text{m}$. Therefore, the FSR is narrowed down to 200 nm in $3.2\text{ }\mu\text{m}$ to $3.4\text{ }\mu\text{m}$ wavelength range, where these gases have distinctive absorption features. This translates into $m = 15$ order of operation with a physical cavity length that varies from $24\text{ }\mu\text{m}$ to $25.5\text{ }\mu\text{m}$.

The reflectivity of the Bragg mirrors increases with the number of high and low refractive index layer pairs as well as the refractive index contrast between the materials. Silicon ($n_{\text{Si}} = 3.61$) and silicon dioxide ($n_{\text{SiO}_2} = 1.45$) are selected as high and low refractive index materials due to their good contrast. A 3-pair mirror with Si and SiO_2 is designed using the transfer-matrix method while taking into account the effect of thick silicon wafer.^{27,28} Since the tapered mirror is fabricated by tapering the first SiO_2 layer, the reflectivity and the transmissivity changes along the length of the mirror. As shown in Fig. 2, the reflectivity of the LVOF varies between 98.5% and 99.5% in the given wavelength range, along the length of the filter.

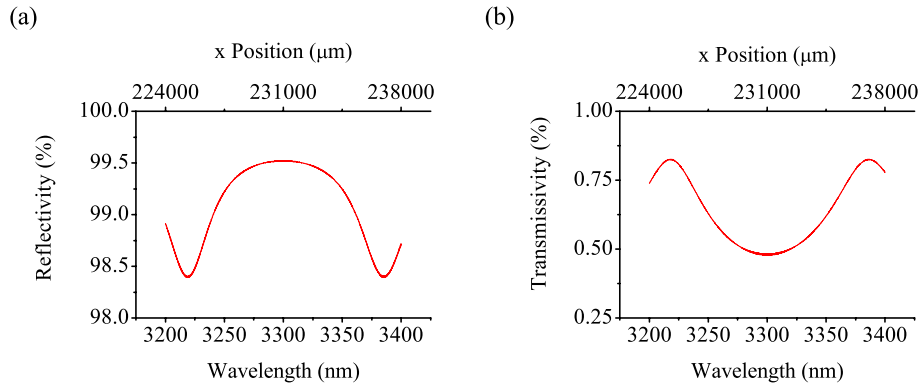


Figure 2. The combined (a) reflectivity and (b) transmissivity of the flat and the tapered Bragg mirrors.

The x-axis shows the position along the length of the filter which is the distance from the wedge apex. It should be noted that in a practical device, the wedge apex is imaginary and an offset is introduced to the x-

position such that the resulting cavity length range covers the spectrum of interest. For a 14 mm long filter with a physical cavity length that varies from 24 μm to 25.5 μm , the desired transmission peaks lie in the 224 mm to 238 mm range, away from the cavity wedge apex.

LVOFs are usually treated as an array of fixed FP filters and the spectral response is calculated assuming parallel mirrors. However, at demanding operating conditions, i.e. high order of operation and highly reflective mirrors, the taper of the cavity cannot be neglected. The difference in the trajectory of the reflected beams between the FP filter and LVOF is illustrated schematically in Fig. 3. Contrary to the constant angle of reflection in the FP filter, the angle of reflection increases with increasing number of reflections at positive angle of incidence in an LVOF. In a similar manner, when the beam is incident towards the wedge apex, i.e. negative angle of incidence, the angle of reflection decreases with increasing number of reflections.

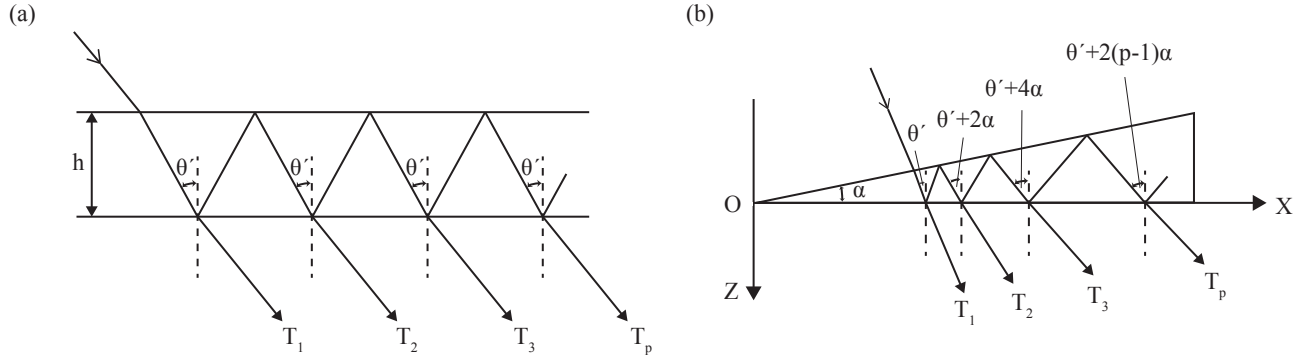


Figure 3. Multiple reflections in (a) Fabry-Perot filter and (b) LVOF at a positive angle of incidence.

The nonparallelism of the mirrors and the resulting change in the angle of reflection in the cavity forces the spectral response of an LVOF to diverge from an FP filter at demanding operating conditions. Due to this effect, the incidence angle of the light beam and the position of the detector plane become optimization parameters. The spectral response of an LVOF has been analyzed using the Fizeau interferometer approach.²⁹ It was shown that for every detector plane position, there exists an angle of incidence, where the narrowest transmission curve with the highest transmittance is achieved.

The spectral response of an LVOF at the 15th order with 3-pair Si-SiO₂ Bragg mirrors is calculated at 3.39 μm wavelength. The spectrum is observed right after the filter and the light beam impinges on the filter at the optimum incidence angle of -1.61° as shown in Fig. 4.

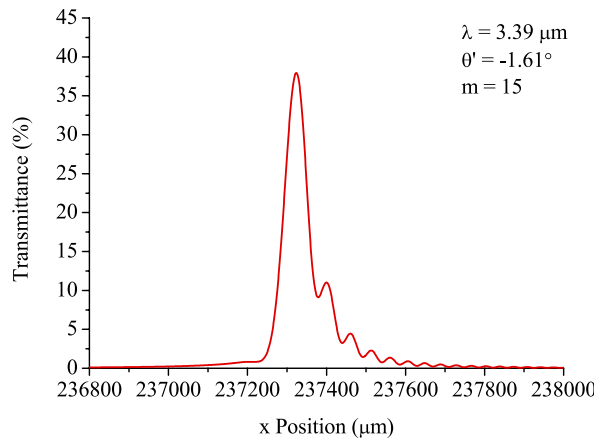


Figure 4. The spectral response of the LVOF at 3.39 μm wavelength, calculated using the Fizeau model with an incidence angle of -1.61° . The filter is scanned along its length and the 15th order is captured.

3. FABRICATION

The fabrication of the gas-filled LVOF is based on direct bonding of the flat and tapered Bragg mirror wafers. The 3-pair Si-SiO₂ flat mirror is sputtered in a 30 μm deep KOH etched cavity. For fabricating the tapered Bragg mirror, the first SiO₂ layer is tapered and the rest of the thin-film layers are sputtered evenly. When these two mirrors are bonded, a tapered cavity is achieved.

The tapered layer is fabricated using a CMOS-compatible method with reflow of a photoresist layer and subsequent transfer etching.³⁰ A 6 μm thick positive photoresist is patterned such that it results in an array of trenches with constant width and linearly variable pitch. Then, the photoresist goes through a thermal-chemical reflow step with propylene glycol monomethyl ether acetate (PGMEA) used as the solving agent at 40 °C. The reflow step transforms the blocks of photoresist into a smooth tapered structure. Lastly, the tapered profile is transferred onto the underlying SiO₂ layer by one-to-one reactive ion etching.

For the proof-of-concept, all of the devices were fabricated with gas inlet and outlet opened with deep reactive ion etching. The profile of a tapered mirror measured before wafer bonding is shown in Fig. 5.

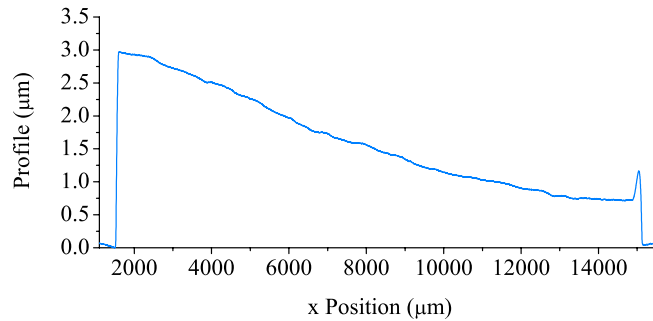


Figure 5. The profile of the tapered mirror measured before wafer bonding. A level difference of 2.2 μm is achieved between the two ends of the mirror, which is enough to cover the spectrum of at least one order.

4. CHARACTERIZATION

The characterization of the gas-filled LVOF relies on individual transmission measurements at several positions along the length of the device. When the filter is scanned along its length with a detector pixel that is narrower than the width of the transmission curve, the spectral response of the device at the wavelength of the light source can be reconstructed. Since the high-finesse interference filters are very sensitive to the collimation of the light source,³¹ a highly collimated mid-IR HeNe laser at 3392 nm wavelength (Research Electro-Optics, Inc., USA) is used for characterization to show the performance of the LVOF as a nondispersive infrared (NDIR) gas sensor.

The actual characterization setup with an HeNe laser is shown in Fig. 6. The light beam coming out of the laser with a negligible full divergence angle of 2.13 mrad passes through the optical chopper. Then, the beam bounces off the beam-steering mirror, which is used for adjusting the incidence angle for optimum operation. Later, the light beam is transmitted through the LVOF and the filtered light is captured by the detector.

A 3 mm tall and 15 μm wide slit is mounted on the large area PbSe detector to replicate a pixel in a detector array. After adjusting the rotational position of the beam-steering mirror for optimum transmission, the detector is aligned with the light beam for maximum throughput. To capture the transmission curve, the filter is scanned along its length via a motorized translational stage with 15 μm steps. At every step, the filter is taken out of the optical light path and a reference measurement is performed. The transmittance is calculated by taking the ratio of the filter and the reference measurements.

To be able to measure the elongation of the optical path through multiple reflections, the sample gas must be kept inside the filter cavity only. To achieve this, dispensing tips are connected to the gas inlet and outlet using silicone. The gas inlet is connected to the sample gas bottle via flexible tubing, while the tube connected to the gas outlet is kept at ambient pressure away from the measurement area. By applying a few mbar of pressure to the sample gas, a pressure difference is generated between the inlet and the outlet; hence, assuring the gas flow through the cavity.

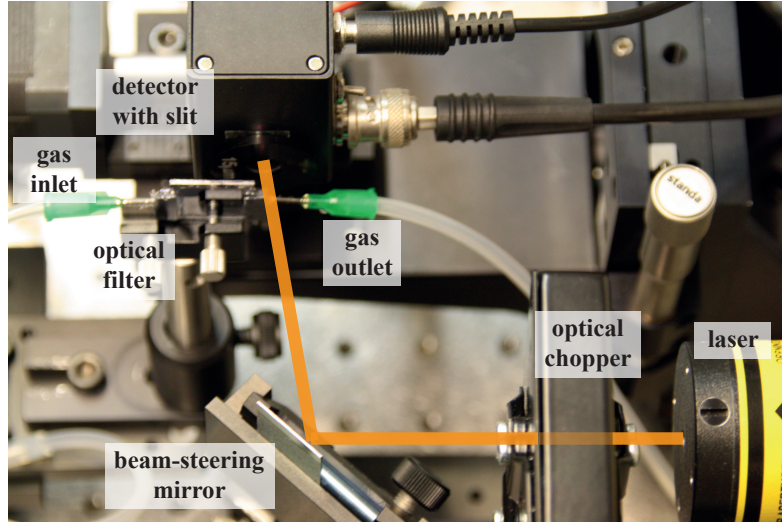


Figure 6. The actual characterization setup for the gas-filled LVOFs.

Considering the distance between the detector and the filter, the optimum incidence angle was found to be -8.8° , experimentally. Since the pressure inside the cavity might cause a slight bending in the mirrors, the sample gas measurement was compared to the infrared-inactive gas at the same pressure, instead of ambient air. The transmittance at 3392 nm wavelength for both the pure sample gas methane and the reference gas nitrogen are measured as shown in Fig. 7.

Methane absorbs almost 80% of the light compared to the reference measurement with nitrogen. To calculate the effective optical path, the absorption coefficient of methane must be evaluated properly. Since the linewidth of the HeNe laser is much narrower than the resolution of the filter, the absorption coefficient must be modified according to the light source. The 200 MHz linewidth of the laser corresponds to an absorption coefficient of $1.0314 \text{ atm}^{-1} \text{ mm}^{-1}$ for methane.^{32,33} Given the modified absorption coefficient, the transmittance of methane translates into an effective optical path of 1.58 mm. When this value is compared to the physical cavity length of $25.44 \mu\text{m}$ that corresponds to the 15th order of operation at 3392 nm wavelength, an elongation factor of 62.2 is calculated.

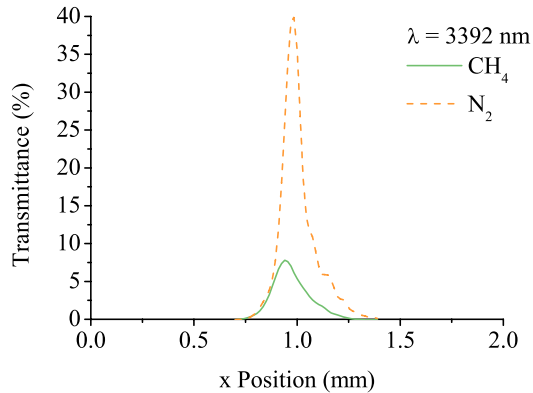


Figure 7. The transmission response of the gas-filled LVOF with methane and nitrogen measured at 3392 nm wavelength.

5. CONCLUSIONS

The proof-of-concept of a gas-filled LVOF has been demonstrated by actual gas measurements. Due to the limited availability of collimated mid-IR light sources, validation in the form of a single-wavelength confirmation as an NDIR gas sensor was performed. Given a well-collimated wideband light source, the LVOF functions as a wideband wavelength-selective device. It was shown that the LVOF must be designed as a Fizeau interferometer at demanding operating conditions, i.e. high order of operation and highly reflective mirrors, where the angle between the mirrors is taken into account. The CMOS-compatible fabrication method was introduced and the measured profile of the tapered mirror showed that the filter covers the desired operating order. The comparison between the gas measurements with methane and nitrogen resulted in an experimental effective optical path of 1.58 mm. This translates into 62.2-fold elongation of a physical cavity length of 25.44 μm, thereby demonstrating the feasibility of the gas-filled LVOF in chip-level miniaturization of spectrometers.

ACKNOWLEDGMENTS

This work has been supported by the Dutch technology foundation STW under grant DEL.11476 and the Energy Delta Gas Research (EDGaR) program. The devices have been fabricated at the Else Kooi Laboratory of TU Delft and the Nanofabrication Laboratory of Chalmers University of Technology.

REFERENCES

- [1] Stuart, B., *[Infrared Spectroscopy: Fundamentals and Applications]*, Wiley (2004).
- [2] Caffey, D., Radunsky, M. B., Cook, V., Weida, M., Buerki, P. R., Crivello, S., and Day, T., “Recent results from broadly tunable external cavity quantum cascade lasers,” *Proc. SPIE* **7953**, 79531K (2011).
- [3] Xu, X., Li, X., Liu, L., and Shang, Y., “High power mid-infrared continuous-wave optical parametric oscillator pumped by fiber lasers,” *Proc. SPIE* **9255**, 925507 (2015).
- [4] Kenda, A., Kraft, M., Tortschanoff, A., Scherf, W., Sandner, T., Schenk, H., Lüttjohann, S., and Simon, A., “Development, characterization and application of compact spectrometers based on MEMS with in-plane capacitive drives,” *Proc. SPIE* **9101**, 910102 (2014).
- [5] Sabry, Y. M., Khalil, D., and Bourouina, T., “Monolithic silicon-micromachined free-space optical interferometers onchip,” *Laser & Photonics Reviews* **9**(1), 1–24 (2015).
- [6] Ayerden, N. P., Aygun, U., Holmstrom, S. T. S., Olcer, S., Can, B., Stehle, J.-L., and Urey, H., “High-speed broadband FTIR system using MEMS,” *Applied Optics* **53**(31), 7267–7272 (2014).
- [7] Manzardo, O., Michaelly, R., Schdelin, F., Noell, W., Overstolz, T., De Rooij, N., and Herzog, H. P., “Miniature lamellar grating interferometer based on silicon technology,” *Optics Letters* **29**(13), 1437–1439 (2004).
- [8] Grabarnik, S., Emadi, A., Wu, H., de Graaf, G., and Wolffenbuttel, R. F., “High-resolution microspectrometer with an aberration-correcting planar grating,” *Applied Optics* **47**(34), 6442–6447 (2008).
- [9] Zimmer, F., Grueger, H., Heberer, A., Wolter, A., and Schenk, H., “Development of a NIR microspectrometer based on a MOEMS scanning grating,” *Proc. SPIE* **5455**, 9–18 (2004).
- [10] Wolffenbuttel, R. F., “State-of-the-art in integrated optical microspectrometers,” *IEEE Transactions on Instrumentation and Measurement* **53**(1), 197–202 (2004).
- [11] Coates, J. P., “New microspectrometers: Building on the principle that simple is beautiful,” (2000).
- [12] Wolffenbuttel, R. F., “MEMS-based optical mini- and microspectrometers for the visible and infrared spectral range,” *Journal of Micromechanics and Microengineering* **15**(7), S145 (2005).
- [13] Neumann, N., Ebermann, M., Kurth, S., and Hiller, K., “Tunable infrared detector with integrated micromachined Fabry-Perot filter,” *Journal of Micro/Nanolithography, MEMS, and MOEMS* **7**(2), 021004 (2008).
- [14] Correia, J. H., Bartek, M., and Wolffenbuttel, R. F., “Bulk-micromachined tunable Fabry-Perot microinterferometer for the visible spectral range,” *Sensors and Actuators A: Physical* **76**(13), 191–196 (1999).
- [15] Swinehart, D. F., “The Beer-Lambert law,” *Journal of Chemical Education* **39**(7), 333 (1962).
- [16] White, J. U., “Long optical paths of large aperture,” *Journal of the Optical Society of America* **32**(5), 285–288 (1942).

- [17] Herriott, D. R. and Schulte, H. J., "Folded optical delay lines," *Applied Optics* **4**(8), 883–889 (1965).
- [18] Thoma, M. L., Kaschow, R., and Hindelang, F. J., "A multiple-reflection cell suited for absorption measurements in shock tubes," *Shock Waves* **4**(1), 51–53 (1994).
- [19] Gagliardi, G. and Loock, H.-P., [*Cavity-Enhanced Spectroscopy and Sensing*], Springer (2014).
- [20] Jackson, D. A., "The spherical Fabry-Perot interferometer as an instrument of high resolving power for use with external or with internal atomic beams," *Proceedings of the Royal Society of London. Series A, Mathematical and Physical Sciences* **263**(1314), 289–308 (1961).
- [21] Kastler, A., "Atomes à l'Intérieur d'un interféromètre Perot-Fabry," *Applied Optics* **1**(1), 17–24 (1962).
- [22] Hernandez, G., "Fabry-Perot with an absorbing etalon cavity," *Applied Optics* **24**(18), 3062–3067 (1985).
- [23] Welzel, S., Lombardi, G., Davies, P. B., Engeln, R., Schram, D. C., and Röpcke, J., "Trace gas measurements using optically resonant cavities and quantum cascade lasers operating at room temperature," *Journal of Applied Physics* **104**(9), 093115 (2008).
- [24] Romanini, D., Chenevier, M., Kassi, S., Schmidt, M., Valant, C., Ramonet, M., Lopez, J., and Jost, H.-J., "Optical-feedback cavity-enhanced absorption: a compact spectrometer for real-time measurement of atmospheric methane," *Applied Physics B* **83**(4), 659–667 (2006).
- [25] Musca, C. A., Antoszewski, J., Winchester, K. J., Keating, A. J., Nguyen, T., Silva, K. K. M., Dell, J. M., Faraone, L., Mitra, P., Beck, J. D., Skokan, M. R., and Robinson, J. E., "Monolithic integration of an infrared photon detector with a MEMS-based tunable filter," *IEEE Electron Device Letters* **26**(12), 888–890 (2005).
- [26] Correia, J. H., de Graaf, G., Kong, S. H., Bartek, M., and Wolffenbuttel, R. F., "Single-chip CMOS optical microspectrometer," *Sensors and Actuators A: Physical* **82**(13), 191–197 (2000).
- [27] Yeh, P., [*Optical Waves in Layered Media*], Wiley (1988).
- [28] Santbergen, R., Smets, A. H. M., and Zeman, M., "Optical model for multilayer structures with coherent, partly coherent and incoherent layers," *Optics Express* **21**(S2), A262–A267 (2013).
- [29] Ayerden, N. P., de Graaf, G., and Wolffenbuttel, R. F., "Compact gas cell integrated with a linear variable optical filter," *Optics Express* **24**(3), 2981–3002 (2016).
- [30] Emadi, A., Wu, H., Grabarnik, S., De Graaf, G., and Wolffenbuttel, R., "Vertically tapered layers for optical applications fabricated using resist reflow," *Journal of Micromechanics and Microengineering* **19**(7), 074014 (2009).
- [31] Ayerden, N. P., Ghaderi, M., de Graaf, G., and Wolffenbuttel, R. F., "Optical design and characterization of a gas filled MEMS Fabry-Perot filter," *Proc. SPIE* **9517**, 95171N (2015).
- [32] Rothman, L. S., Gordon, I. E., Barbe, A., Benner, D. C., Bernath, P. F., Birk, M., Boudon, V., Brown, L. R., Campargue, A., Champion, J. P., Chance, K., Coudert, L. H., Dana, V., Devi, V. M., Fally, S., Flaud, J. M., Gamache, R. R., Goldman, A., Jacquemart, D., Kleiner, I., Lacome, N., Lafferty, W. J., Mandin, J. Y., Massie, S. T., Mikhailenko, S. N., Miller, C. E., Moazzen-Ahmadi, N., Naumenko, O. V., Nikitin, A. V., Orphal, J., Perevalov, V. I., Perrin, A., Predoi-Cross, A., Rinsland, C. P., Rotger, M., imekov, M., Smith, M. A. H., Sung, K., Tashkun, S. A., Tennyson, J., Toth, R. A., Vandaele, A. C., and Vander Auwera, J., "The HITRAN 2008 molecular spectroscopic database," *Journal of Quantitative Spectroscopy and Radiative Transfer* **110**(910), 533–572 (2009).
- [33] Semiletova, E., Arshinov, Y., Mikhailenko, C., Babikov, Y., and Golovko, V., "Information-calculating system spectroscopy of atmospheric gases. the structure and main functions," *Atmospheric and Oceanic Optics* **18**(9), 685 (2005).